

Valence-band structure of TiC and TiN

L. I. Johansson*

Stanford Synchrotron Radiation Laboratory, Stanford, California 94305

P. M. Stefan and M. L. Shek

Stanford Electronics Laboratories, Stanford University, Stanford, California 94305

A. Nørnlund Christensen

Department of Chemistry, Aarhus University, DK-8000 Aarhus C, Denmark

(Received 22 October 1979)

The valence-band structure of single crystals of titanium carbide (TiC) and titanium nitride (TiN) have been studied with angle-integrated photoelectron spectroscopy using He I, He II, and synchrotron radiation for excitation. The results are compared with the partial densities of states derived from an augmented-plane-wave band-structure calculation. Peak positions and widths agree fairly well, but the observed intensity modulations with photon energy cannot be interpreted by such a comparison.

INTRODUCTION

The exceptional combination of physical properties displayed by transition-metal carbides and nitrides is closely connected with their electronic band structure. These compounds have, therefore, been a subject of special interest theoretically, particularly with regard to their electronic structure.¹⁻⁸ The most intensively studied compound among these is TiC, which has been closely examined both theoretically¹⁻¹¹ and experimentally.^{4,7,8,12-16} The controversy between the earliest linear-combination-of-atomic-orbitals (LCAO)⁸ and augmented-plane-wave (APW)^{2,3} calculations regarding the direction of charge transfer and the location of the C 2s band has been resolved. The most recent experimental results^{4,7,12-15} all essentially confirm the results of the APW calculations, which predict electron charge transfer from titanium to carbon. They also locate the C 2s band at about 11 eV below the Fermi level, with the result that the C 2s band is well separated from the band caused by hybridization between C 2p and Ti 3d states, which extends down to about 7 eV below the Fermi level.

To date the most detailed experimental valence-band information (highest energy resolution) has been obtained using x-ray^{4,12,13} and uv (Ref. 13) photoelectron spectroscopy (XPS and UPS). Comparisons between XPS valence-band spectra and calculated density of states (DOS), which has been convoluted with the instrumental response function, have yielded very satisfactory results for the relative positions of the valence-band peaks.^{4,5,9-11} The intensities are more difficult to interpret,⁹ however, because of effects of the surface, transition matrix elements and uncertainties in the final-state approximation. In order

to supply new, detailed experimental information about the valence-band structure of TiC and TiN we have performed a photoemission experiment using synchrotron radiation supplemented with He I and He II radiation. For both TiC and TiN, the hybridization band consists of 3d and 2p states. Therefore, even though the photoionization cross section of these states changes substantially over the photon energy range used (21–190 eV), no dramatic changes in the valence-band spectra are expected since neither state exhibits a so-called Cooper minimum in the cross section.

Thus one cannot hope to directly disentangle the contribution of the two different states in these cases. The present results, in particular the evolution of the valence-band spectra with photon energy, will hopefully serve as input data for future interpretations of peak intensities, which take into account the roles of the various effects mentioned above. For TiN a comparison between the calculated DOS and high-resolution, valence-band photoelectron spectra is made for the first time.

EXPERIMENTAL

Preparation of single crystals

Single crystals of TiC were made using a vertical floating-zone technique¹⁷ and the procedure previously described.¹³ The starting materials for the crystal growth experiments were hot-pressed rods which, prior to the zone melting, had the composition Ti: 77.7, C: 18.62, O: 0.04, N: 0.89, W: 2.5, Fe: 0.023, Co: 0.003 at. %. All numbers indicate weight %, and are the results of a chemical analysis performed by the supplier (Dr. B. O. Haglund, Sandvik AB, Stockholm, Sweden). After zone melting, the single crystals of

TiC had the composition $\text{Ti}_{0.98(3)}\text{C}_{1.0}$, according to a neutron-diffraction determination of the structure and composition.¹⁸ The composition of this specimen is thus stoichiometric within experimental errors.

Single crystals of TiN could not be obtained by the technique used for TiC. A new technique was developed to prepare TiN from titanium and nitrogen with crystal growth occurring in a single operation. This was achieved using a zone-annealing technique. In zone annealing, the sample is heated to a temperature below the melting point of the material. The starting materials for the crystal-growth experiments were bars of titanium (approximately 150 mm long and 6 mm in diameter) of nominal purity 99.9%, and nitrogen gas of the nominal purity 99.99%. The crystals were grown at a nitrogen gas pressure of up to 2 MPa in the same crystal-growth furnace as used for TiC. Before each growth experiment, the furnace was evacuated three times to a vacuum < 1 Pa before the final ambient gas pressure was adjusted. The specimens were held vertically in holders of boron nitride and travelled downwards relative to the heating coil. The growth rate, defined as the travel speed of the specimen, was in the range 2 to 9 mm h⁻¹. The temperature of the heated zone was approximately 2600 °C.

By using the zone-annealing technique specimens with large single-crystal grains of TiN were obtained. The composition of the specimens was determined by gravimetric analysis. TiN was converted quantitatively to TiO_2 by ignition in air at 1000 °C. The samples were placed in Pt crucibles and kept in an electric furnace for approximately 1 h. The composition of the samples investigated was $\text{TiN}_{0.83}$. In the following discussion the formula TiN is used for this nonstoichiometric specimen.

Disks were cut from the specimens of TiC and TiN using a spark erosion technique. The crystals were aligned along crystallographic directions to better than $\pm 0.5^\circ$ using the Laue back-reflection technique and disks were cut parallel to the (100), (110), and (111) planes. The misalignment of the crystal surfaces studied relative to the crystallographic directions was less than 2° . The Laue pattern did not indicate the presence of any powder in the samples used in these experiments. The crystals were polished and rinsed in ethanol before being mounted in the photoemission apparatus. For the studies presented below, one TiC (110) crystal and one TiN (100) crystal were used.

Experimental procedure

In situ cleaning of the crystal surfaces was a crucial step in performing these studies, since

even small amounts of a residual surface contaminant, such as oxygen would interfere severely when using low-energy photons. When using x rays one is not particularly sensitive to oxygen adsorbed on the sample surface as has been demonstrated in previous XPS studies of the valence-band structure of TiC.^{4,12} This is because the electron escape depth is considerably larger for energies in the 1.0–1.5 keV range than in the 40–200 eV range.¹⁹ In addition, the $\text{O}2p/\text{Ti}3d$ photoionization cross section ratio is smaller at the high photon energies.²⁰ Consequently, a cleaning procedure more effective than any previously reported had to be accomplished.

Since high-temperature flashings *in situ* had been found effective against some surface contaminants on a WC crystal,²¹ this technique was adopted for TiC and TiN as well. It is a method that does not seem to produce undesirable changes in surface composition and structure as may be the case when utilizing ion bombardment or scraping techniques. The experimental chamber used had a base pressure of $< 1.0 \times 10^{-8}$ Pa. After outgassing and repeated flashings at increasing temperatures, the final flashings (5–10 sec) could be done while keeping the pressure on the 10^{-8} Pa scale. The cleanliness of the samples was checked with Auger electron spectroscopy (AES). It was found that flashings to about 1700 °C for TiC, and to about 1400 °C for TiN, were necessary to drive off residual sulphur and oxygen. AES spectra of our best efforts to clean the TiC and TiN crystals are shown in Fig. 1. The carbide C KLL Auger peak (around 270 eV) and the Ti LMM peaks (between about 350–450 eV) characterize the TiC spectrum. No sulphur or oxygen peaks are discernible but a weak W signal is seen around 180 eV. In the TiN spectrum the NKLL and Ti LMM signals overlap each other. In this case a very weak oxygen signal remained, as seen around 510 eV, but this amount was sufficiently small

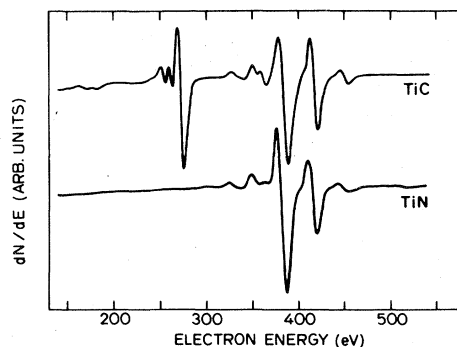


FIG. 1. AES spectra of clean TiC and TiN crystals obtained using a 2-keV electron beam for excitation.

so that no O 2*p* peak appeared and interfered in the photoemission results. The crystal structure was checked after the cleaning procedure and the crystals were found to produce very good LEED patterns.

Photoemission measurements were performed using monochromatized He I (21.2 eV) and He II (40.8 eV) radiation²² and synchrotron radiation from the 4° branch line²³ of Beam Line I at the Stanford Synchrotron Radiation Laboratory. The emitted electrons were energy analyzed in a double-pass cylindrical mirror analyzer. The analyzer was operated in the retarding²⁴ mode and at an energy resolution of 0.40 eV. The analyzer was located so its optical axis was lying in the incidence plane of the linearly polarized synchrotron radiation but at an angle of 75° relative to the incidence direction. The samples were positioned so that the surface normal coincided (within a few degrees) with the optical axis of the analyzer. Thus, the results presented below represent angle-integrated data, integrated over polar angles between 36° and 48°. The midpoint of the Fermi edge has been used as the reference level in all spectra.

RESULTS AND DISCUSSION

Valence-band spectra of TiC induced by He I and He II radiation are shown in Fig. 2. The structure observed between 0 and 7 eV below the Fermi level (E_F) arises from hybridized Ti 3*d* and C 2*p* states. Maximum intensity is obtained at 2.9 eV below E_F and the shoulder on the high binding-energy side appears around 5 eV. In the He II spectrum a broad peak around 11 eV below E_F is also observed which originates from C 2*s* states. The

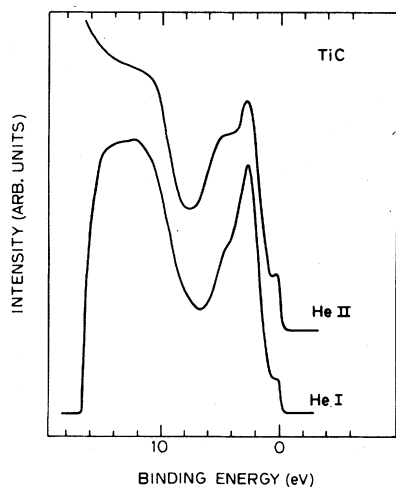


FIG. 2. Valence-band spectra of TiC induced by He I and He II radiation.

He I spectrum closely reproduces previously published results,¹³ but our He II spectrum looks distinctly different. This is most probably due to the fact that a more effective cleaning procedure was employed in our case and that we could monitor the surface cleanliness to make sure that no contaminants, such as oxygen or sulphur, remained on the surface. It should be pointed out that the photoemission technique is extremely surface sensitive in the 40–150 eV energy range, since the electron escape depth exhibits a minimum in this range.¹⁹ The apparently large number of secondary electrons obtained in the spectra is mainly due to the transmission properties of the cylindrical mirror analyzer since its efficiency varies as E_p^2/E_{kin} when operated in the retarding mode²⁴ (E_p is the pass energy of the analyzer and E_{kin} is the kinetic energy of the analyzed electron).

Valence-band spectra of TiN induced by He I and He II radiation are shown in Fig. 3. In this case, structures interpreted as arising from hybridized Ti 3*d* and N 2*p* states are observed down to a binding energy of about 9 eV. A distinct peak appears just below E_F and a minimum is observed around 2.5 eV. The most intense structure, lying between 2.5 and 9 eV, exhibits a maximum at 5.0 eV below E_F and a shoulder at a binding energy of about 7 eV. In the He II spectrum, a broad structure around 16 eV is also observed, which we interpret as originating from N 2*s* states.

Synchrotron radiation induced valence-band spectra of TiC and TiN are shown in Figs. 4 and 5, together with the partial densities of states calculated by an LCAO interpolation scheme on a self-consistent APW band-structure calculation.¹ For the recorded spectra, the relative photon flux and the analyzer efficiency have been normalized out so the intensities are shown in relative units. By including the multiplication factor given for each curve the "true relative" intensity variation

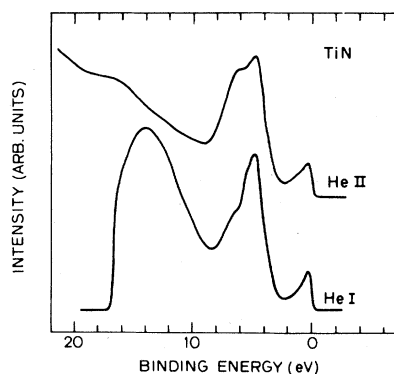


FIG. 3. Valence-band spectra of TiN induced by He I and He II radiation.

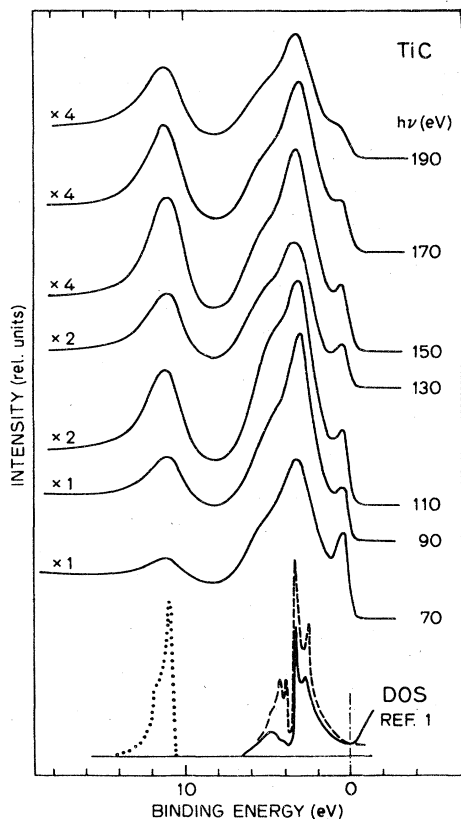


FIG. 4. Valence-band spectra of TiC induced by synchrotron radiation. The spectra have been normalized with respect to variations in incident photon flux and energy analyzer transmission efficiency. Also shown are calculated partial densities of states (Ref. 1). Dotted curve, DOS of C 2s; dashed curve, DOS of C 2p; solid curve, DOS of Ti 3d.

with photon energy is shown. Therefore Figs. 4 and 5 illustrate directly how the valence-band spectra of TiC and TiN evolve with photon energy.

Let us first discuss the TiC spectra in Fig. 4. The strongest effect observed in the valence-band spectrum upon increasing the photon energy from 70 to 190 eV is seen to be an increase in the relative strength of the C 2s peak, located about 11 eV below E_F . This is exactly what was expected based on previous XPS (Refs. 4, 12, 13) and UPS (Ref. 13) results on TiC as well as on the calculated energy dependence of the atomic photoionization cross section for C 2s states compared to Ti 3d and C 2p states.²⁰ The effects on the structure arising from hybridized Ti 3d and C 2p states is not so clear cut, however. The general shape of this structure remains constant but some intensity modulations of particular spectral features are seen to occur in the photon energy range 70–130 eV. The Fermi edge shoulder is more pronounced in the 70-eV spectrum than for the other photon

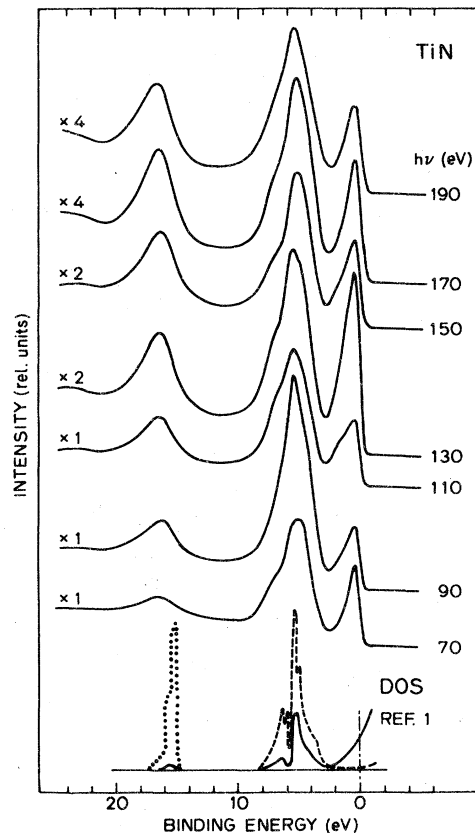


FIG. 5. Valence-band spectra of TiN induced by synchrotron radiation. The spectra have been normalized with respect to variations in incident photon flux and energy analyzer transmission efficiency. Also shown are calculated partial densities of states (Ref. 1). Dotted curve, DOS of N 2s; dashed curve, DOS of N 2p; solid curve, DOS of Ti 3d.

energies and the peak maximum is most prominent in the 90-eV spectrum.

In comparing the experimental results with the calculated partial densities of states,¹ one finds that the calculation gives a good prediction of the locations of the peak maxima at 3.0 (± 0.2) eV and 11.2 (± 0.3) eV, as well as of the width of the structure arising from the hybridized C 2p, Ti 3d bands (≤ 7 eV). Cluster calculations using MO (molecular orbital) methods have shown a similarly good agreement in the positions of spectral details for TiC (and ZrC) valence bands when XPS spectra are compared with the calculated total density of states.¹⁰ In Fig. 4, the C 2p (dashed curve) and Ti 3d (solid curve) partial densities of states are seen to overlap each other completely and are moreover seen to have essentially the same shape. This prevents any simple interpretation of the observed intensity modulations based on the different energy dependence of 2p and 3d photoionization cross sections. Thus a rigorous theoretical analysis accounting

for the effects of transition matrix elements and final states seems necessary for an interpretation of the intensity modulations within the hybridization band.

One thing to notice about the spectra presented in Figs. 4 and 5 is that the overall energy resolution decreases slightly at the higher photon energies. The halfwidth of the monochromatic radiation is given (in eV) by $\Delta E = 8 \times 10^{-6} (h\nu)^2$ when a 1200 lines/mm grating is used.²⁵ This means that in our case the radiation starts to make a non-negligible contribution to the total observed broadening at the higher photon energies. The resolution of the electron analyzer was kept constant at 0.40 eV throughout the measurements.

Comparison between the experimental and calculated results for TiN (Fig. 5) leads to several important observations. First, the calculated results predict the following features of the hybridized band rather well: (1) a double-peaked valence band with a minimum around 2.5 eV below E_F ; (2) a bandwidth of 9 eV; and (3) a peak and a shoulder located at 5.3 (± 0.3) eV and around 7 eV, respectively. Regarding the N2s level, however, the calculation locates it at a binding energy that is about 1 eV smaller than what is obtained experimentally, 16.4 (± 0.3) eV. The changes seen in the TiN valence-band spectra, upon increasing the photon energy from 70 to 190 eV, are essentially similar to those observed for TiC. As is the case for C2s, the relative strength of the N2s peak increases with increasing photon energy. But in comparison with TiC, stronger intensity modulations within the hybridization band are observed between 70–150 eV. In this case the N2p (dashed curve) and Ti3d (full curve) densities of states have different shapes (see Fig. 5) which lead us to assume that the structure observed just below the Fermi level is derived from Ti3d states. A maximum in the N2p photoionization cross section around 90 eV would then explain the modulations seen between 70 and 110 eV. However, an anomaly appears in the 130-eV spectrum in which the structure closest to the Fermi level, and assigned to Ti3d states, has a peak intensity comparable to that of the structure between 2.5 and 9 eV below E_F . The energy level diagram of TiN is such that enhancement effects due to $3p \rightarrow 3d$ absorption transitions are excluded.²⁶ Therefore other explanations must be sought. An obvious one is that we have discussed the spectra only in terms of initial densities of states. Constant transition matrix elements and a complete angle averaging have implicitly been assumed. For the photon energies used, however, this is a poor assumption, since significant effects due to matrix elements and the final-state band structure may occur.²⁷ We are,

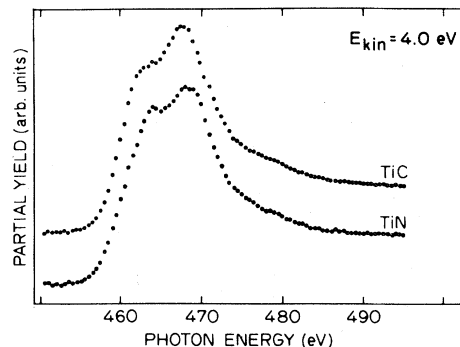


FIG. 6. Partial electron yield spectra of TiC and TiN over the Ti L -absorption region.

moreover, only integrating over polar angles between about 36° and 48° . Since no band-structure calculation has been carried out to such high energies and the experimental time available to us did not allow a closer examination of how the band structure of TiN evolves for photon energies between 110–150 eV, we cannot, at present, provide an interpretation of the 130-eV spectrum.

The observed width of the 2s band is significantly broader both for TiC and TiN than that predicted. Full widths of about 5 eV and 6 eV are obtained for TiC and TiN, respectively, while the calculated bandwidths are 3.3 and 2.4 eV, respectively.¹ The same observation has previously been made in XPS spectra of carbides and was suggested to be due to lifetime broadening.^{4,5}

We also studied the absorption coefficient near the $L_{II,III}$ edges utilizing the partial electron yield technique.²⁸ The results are shown in Fig. 6. A pronounced peak, split into a doublet, is observed just above threshold. The splitting is about 5 eV and is in fair agreement with the spin-orbit splitting of 6.0 eV observed between the $2p_{3/2}$ – $2p_{1/2}$ levels in XPS spectra of TiC.¹² The “white line” character of the absorption coefficient near the $L_{II,III}$ thresholds has previously been investigated for Ti metal²⁹ and can be understood also for TiC and TiN in terms of a high density of empty d -derived states immediately above E_F . What significance can be attributed to the small shift in peak positions between TiC and TiN (~ 0.5 eV) is not clear, due to the strong perturbation by the conduction electrons of the hole states near threshold, as pointed out in previous work.²⁹

In summary, our experimental results have given new detailed information about the band structure of TiC and TiN, and how the valence-band spectra evolve with photon energy. A comparison to calculated partial densities of states explains the origin of the observed spectral features and the agreement in peak positions and widths is fairly good. To interpret the observed intensity mod-

ulations within the hybridized $2p$, $3d$ bands, however, a rigorous theoretical analysis seems necessary. For gaining further insight into the detailed band structure of these compounds, an angle-resolved photoemission study is desirable.

ACKNOWLEDGMENTS

We would like to thank Professor I. Lindau and Professor W. E. Spicer for letting us use their

photoemission equipment for these experiments. Carlsberg Fondet is acknowledged for supplying a spark erosion machine for the crystal growth project. The experiments were performed at the Stanford Synchrotron Radiation Laboratory, which is supported by the National Science Foundation under Contract No. DMR 77-27489 in cooperation with the Stanford Linear Accelerator Center and the Department of Energy.

*Present address: Department of Physics and Measurement Technology, Linköping University, S-581 83 Linköping, Sweden.

¹A. Neckel, P. Rastl, R. Eibler, P. Weinberger, and K. Schwarz, *J. Phys. C* **9**, 579 (1976).

²V. Ern and A. C. Switendick, *Phys. Rev.* **137**, A1927 (1965).

³J. B. Conklin, Jr. and D. J. Silversmith, *Int. J. Quantum Chem.* **11S**, 243 (1968).

⁴H. Ihara, Y. Kumashiro, and A. Itoh, *Phys. Rev. B* **12**, 5465 (1975).

⁵H. Ihara, M. Hirabayashi, and H. Nagagawa, *Phys. Rev. B* **14**, 1707 (1976).

⁶H. R. Trebin and H. Bross, *J. Phys. C* **8**, 1181 (1975).

⁷J. F. Alward, C. Y. Fong, M. El-Batanouny, and F. Wooten, *Phys. Rev. B* **12**, 1105 (1975).

⁸R. G. Lye and E. M. Logothetis, *Phys. Rev.* **147**, 622 (1966).

⁹P. Weinberger, *Theor. Chim. Acta* **44**, 315 (1977).

¹⁰V. A. Gubanov, A. L. Ivanovskii, G. P. Shveikin, and J. Weber, *Solid State Commun.* **29**, 743 (1979).

¹¹A. L. Ivanovskii, V. A. Gubanov, E. Z. Kurmayev, A. L. Hagström, S.-E. Karlsson, and L. I. Johansson, *J. Electron Spectrosc. Relat. Phenom.* **16**, 415 (1979).

¹²L. I. Johansson, A. L. Hagström, B. E. Jacobson, and S. B. M. Hagström, *J. Electron Spectrosc. Relat. Phenom.* **10**, 259 (1977).

¹³A. L. Hagström, L. I. Johansson, S. B. M. Hagström, and A. N. Christensen, *J. Electron Spectrosc. Relat. Phenom.* **11**, 75 (1977).

¹⁴J. F. Alward, C. Y. Fong, M. El-Batanouny, and F. Wooten, *Solid State Commun.* **17**, 1063 (1975).

¹⁵S. Manninen and T. Paakkari, *J. Phys. C* **9**, 95 (1976).

¹⁶For references to earlier work see the references given in Ref. 13.

¹⁷A. N. Christensen, *J. Cryst. Growth* **33**, 99 (1976).

¹⁸A. N. Christensen, *Acta Chem. Scand.* **A29**, 563 (1975).

¹⁹I. Lindau and W. E. Spicer, *J. Electron Spectrosc. Relat. Phenom.* **3**, 409 (1974).

²⁰E. J. McGuire, Sandia Laboratories, Albuquerque, New Mexico, Technical Report No. SC-RR-70-721 (1970); J. H. Scofield, *J. Electron Spectrosc. Relat. Phenom.* **8**, 129 (1976).

²¹P. M. Stefan, L. I. Johansson, M. L. Shek, I. Lindau, G. Brogren, and W. E. Spicer (unpublished).

²²J. N. Miller, thesis, Stanford University, 1979 (unpublished).

²³F. C. Brown, B. Bachrach, and N. Lien, *Nucl. Instrum. Methods* **152**, 72 (1978).

²⁴P. W. Palmberg, *J. Vac. Sci. Technol.* **12**, 379 (1975).

²⁵Experience has shown that the width is about twice the theoretical width given in Ref. 23.

²⁶See, for example, C. Guillot, Y. Ballu, J. Paigue, J. Lecante, K. P. Jain, P. Thiry, R. Pinchaux, Y. Petroff, and L. M. Falicov, *Phys. Rev. Lett.* **39**, 1632 (1977).

²⁷J. Stöhr, G. Apai, P. S. Wehner, F. R. McFeely, R. S. Williams, and D. A. Shirley, *Phys. Rev. B* **14**, 5144 (1976).

²⁸G. J. Lapeyre, R. J. Smith, and I. Andersson, *J. Vac. Sci. Technol.* **14**, 384 (1977).

²⁹D. Denley, R. S. Williams, P. Perfetti, D. A. Shirley, and J. Stöhr, *Phys. Rev. B* **19**, 1762 (1979).